Proceedings of the 20th International Conference on Soil Mechanics and Geotechnical Engineering– Rahman and Jaksa (Eds)

Thermo-mechanical load transfer mechanism of energy piles

Mécanisme de transfert de charge thermomécanique des piles d'énergie

Dunja Perić & Arash Saeidi Rashk Olia
Department of Civil Engineering, Kansas State University, U.S.A., peric@ksu.edu

ABSTRACT: In this study recently derived analytical solutions for soil structure interaction in energy piles are implemented to investigate load transfer mechanisms of energy piles subjected to combined thermo-mechanical loads. To this end, end bearing and fully floating energy piles were subjected to complete heating-cooling cycles combined with compressive axial loads. Evolution of the ratio of amount of a force transferred to the soil at the pile tip to the force transferred along the shaft throughout the heating-cooling cycle was obtained for end bearing piles. Similarly, evolution of the ratio of amount of a force transferred to the soil along the bottom portion of the shaft to the top portion of the shaft throughout the heating-cooling cycle was obtained for fully floating piles. Based on these results it was found that during cooling end bearing piles can develop a complete shaft transfer whereby no force is transferred at the pile tip. In addition, end bearing piles during heating can develop a complete tip transfer whereby no force is transferred to the soil along the pile shaft. It was also found that fully floating piles can reach stages whereby the entire load transfer occurs along either the top half or the bottom half of the shaft. The former emerges during cooling, while the latter develops during heating.

RÉSUMÉ : Dans cette étude, des solutions analytiques récemment dérivées pour l'interaction de la structure du sol dans les pieux énergétiques sont mises en œuvre pour étudier les mécanismes de transfert de charge des pieux énergétiques soumis à des charges thermomécaniques combinées. À cette fin, les pieux d'appui d'extrémité et les pieux énergétiques entièrement flottants ont été soumis à des cycles complets de chauffage-refroidissement combinés à des charges axiales de compression. L'évolution du rapport de la quantité d'une force transférée au sol à la pointe du pieu à la force transférée le long du puits tout au long du cycle de chauffage-refroidissement a été obtenue pour les pieux porteurs d'extrémité. De même, l'évolution du rapport de la quantité d'une force transférée au sol le long de la partie inférieure du puits à la partie supérieure du puits tout au long du cycle de chauffage-refroidissement a été obtenue pour des pieux entièrement flottants. Sur la base de ces résultats, il a été constaté que pendant le refroidissement, les pieux porteurs d'extrémité peuvent développer un transfert d'arbre complet par lequel aucune force n'est transférée à la pointe du pieu. De plus, les pieux porteurs d'extrémité pendant le chauffage peuvent développer un transfert de pointe complet par lequel aucune force n'est transférée au sol le long de la tige du pieu. Il a également été constaté que les pieux entièrement flottants peuvent atteindre des stades où tout le transfert de charge se produit le long de la moitié supérieure ou de la moitié inférieure du puits. Le premier émerge lors du refroidissement, tandis que le second se développe lors du chauffage.

KEYWORDS: End restraints, energy piles, load transfer mechanism, soil structure interaction, thermo-mechanics

1 INTRODUCTION

Energy piles are multifunctional, sustainable, energy saving, and environmentally friendly deep foundations. In addition to transferring structural loads to the subsurface, they also enable exchange of renewable thermal energy between the subsurface and superstructure. The low enthalpy thermal energy is used for supplemental space heating and cooling, resulting in a decreased use of fossil fuels and reduced carbon dioxide emissions.

Free deformation of energy piles subjected to temperature changes is restrained due to the presence of the surrounding soil and rock. This results in additional thermally induced displacements, strains and stresses in energy piles. Qualitative and quantitative understanding of a thermo-mechanical soil structure interaction and accompanying induced displacements, strains and stresses are vitally important for analysis, design and wider use of energy piles, thus contributing to the increased sustainability of civil infrastructure.

Energy piles differ from traditional piles in in that the thermal load continuously changes while they are in use. This results in a cyclic loading that is comprised of heating-cooling cycles combined with the approximately constant mechanical load. Previously researchers provided load transfer diagrams for a fully floating energy pile based on the experimental observations of full-scale in situ tests (Bourne-Webb et al. 2009, Amatya et al. 2012, and Bourne-Webb et al. 2013). Their diagrams employed a constant shaft resistance assumption throughout the pile depth, which led to a linear variation of axial force and strain with depth, while axial displacement of a pile was not included. Rotta Loria and Laloui (2018) presented load transfer schemes for fully floating and semi floating energy piles based on thermo-elasticity while pointing out that load diagrams provided by Bourne-Webb et al. (2009) and Bourne-Webb et al. (2013) were not fully explained. Rotta Loria and Laloui (2018) presented the load transfer schemes for the fully floating energy pile without head restraint and semi-floating piles with and without head restraint subjected to thermal, mechanical, and thermo-mechanical loads. They depicted mechanically induced axial stresses with linear distribution versus depth while thermally induced stress was following a non-linear pattern. While they also provided mechanically and thermally induced shear stresses as constant and linear versus depth respectively, no analytical expressions were provided for the quantifying these schemes.

Numerous numerical and experimental studies were conducted with the aim of advancing the knowledge of the soil structure interaction in energy piles while analytical approaches have emerged only recently (Cossel 2019, Perić et al. 2020, Iodice et al. 2020, Saeidi Rashk Olia and Perić 2021a), All these references, except Saeidi Rashk Olia and Perić(2021a) address energy piles embedded in layered soils.

It is noted that the analytical approach can simultaneously provide both, qualitative and quantitative understanding. Consequently, the analytical approach is selected herein for advancing the knowledge of the load transfer mechanism during a full heating-cooling cycle combined with a constant compressive axial load. The loads are applied to end bearing and

fully floating energy piles. The results are obtained by implementing recently derived analytical solutions (Saeidi Rashk Olia and Perić 2021a) for a single energy pile embedded in a homogeneous soil. Details of implementation are discussed below. The unique contribution of this study is in quantifying the evolution of the ratio of end bearing and shaft friction throughout the full heating-cooling cycle combined with compressive axial load. This is accompanied with corresponding free body diagrams of the pile and normalized diagrams depicting the evolution of axial stresses in the pile and shear stresses at the soil pile interface, thus providing in depth understanding of the underlying load transfer mechanisms.

2 ANALYTICAL SOLUTIONS

Perić et al. (2020), and Saeidi Rashk Olia & Perić (2021a) presented analytical solutions for vertical displacement, stress and strain in a single energy pile embedded in layered and homogeneous soils respectively, and subjected to thermo-mechanical loads. The solutions are based on the assumptions of elastic soil-pile interface and a thermo-elastic pile. These assumptions were confirmed by Knellwolf et al. (2011), and Perić et al. (2017). Furthermore, Perić et al. (2020) and Saeidi Rashk Olia and Perić (2021a) successfully validated their analytical solutions against a full scale energy pile test (Laloui et al. 2006) and geotechnical centrifuge test results (Stewart & McCartney 2014, Goode & McCartney 2015), thus fully justifying these assumptions.

The solutions were derived by enforcing the equilibrium of an infinitesimal pile segment in the vertical direction. Based on the restraint conditions at a pile tip the piles were categorized as end bearing and semi floating. In the former case no displacement occurs at the pile tip while in the latter case both displacement and stress develop at the pile tip. An ideally fully floating pile would develop zero stress at the pile tip, thus requiring an infinite length. Nevertheless, a semi floating pile will exhibit a very similar behavior to the ideally fully floating pile in case of an extremely small stress t at the tip. This type of semi floating pile is referred to as fully floating in this study.

The solutions for axial displacement and stress in an end bearing pile embedded in a homogeneous soil layer, subjected to a combined thermo-mechanical load given by Saeidi Rashk Olia & Perić (2021a) are given by Eqs. (1) & (2) respectively.

$$u(x) = \frac{F\sinh(\psi x)}{AE\psi\cosh(\psi L)} + \frac{\alpha\Delta T\sinh(\psi x)}{\psi\cosh(\psi L)} \tag{1}$$

$$\sigma(x) = \frac{F\,cosh(\psi x)}{\mathrm{A}\cosh(\psi L)} + E\alpha\Delta T\left(\frac{\cosh(\psi x)}{\cosh(\psi L)} - 1\right) \tag{2}$$

Eqs. (3) & (4) were also given by Saeidi Rask Olia & Perić (2021a). They provide the thermo-mechanical axial displacement and stress in a fully floating energy pile.

$$u(x) = \frac{F\cosh(\psi x)}{AE\psi sinh(\psi L)} + \frac{\alpha\Delta T sinh\left[\psi\left(x-\frac{L}{2}\right)\right]}{\psi\,\cosh\psi\left(\frac{L}{2}\right)} \tag{3}$$

$$\sigma(x) = \frac{F\sinh(\psi x)}{A\sinh(\psi L)} + E\alpha\Delta T\left(\frac{\cosh\left[\psi\left(x-\frac{L}{2}\right)\right]}{\cosh\psi\left(\frac{L}{2}\right)} - 1\right) \tag{4}$$

u and σ are the axial displacement and stress in the energy pile respectively whereby positive displacement is directed upward, and tensile strains and stresses are positive. Positive x is directed upward with zero value at the pile tip. α represents the coefficient of thermal expansion of the pile, E is the elastic modulus of the pile, ΔT is the temperature difference between the pile and surrounding soil, while A and L are the cross-section area and length of the pile respectively. F is the axial load applied at the pile head that is negative in compression. A parameter ψ represents the pile geometry and relative stiffness of the soil with respect to the pile. It is given by

$$\psi^2 = \left(\frac{p}{A}\right)\left(\frac{k_s}{E}\right) = \xi_g\xi_s \tag{5}$$

whereby p represents the pile perimeter, and k_s is the elastic stiffness of the shear spring that is constant versus depth and attached to the pile shaft. Furthermore, the ratio of p and A is denoted by ξg, and ratio of k_s and E is denoted by ξs.

3 MECHANICS BASED LOAD TRANSFER MECHANISM

3.1 *Load transfer mechanism in end bearing energy piles*

End restraints of the pile plays an important role in thermo-mechanical behavior of energy piles. Saeidi Rashk Olia and Perić (2021b) described end bearing, semi floating and fully floating energy piles. In an end bearing pile load is transferred along both, pile shaft and the pile tip. While the former occurs through shear stress along the soil-pile interface the latter induces normal stress at the pile tip (x =0). As the soil-pile interface is modeled with a linear elastic shear spring, the shear stress along the shaft $\tau = \tau(x)$ is given by

$$\tau(x) = -k_s u(x) \tag{6}$$

where negative sign implies that the shaft resistance acts in the direction opposite to the direction of the axial displacement of the pile. It is because thermal load (ΔT) inherently changes with time while mechanical load imposed by a superstructure is approximately constant that Perić et al. (2020) developed the concept of an equivalent thermal load (ΔT_{eq}). It is defined by

$$\Delta T_{eq} = \frac{F}{AE\alpha} \tag{7}$$

This concept enables transformation of mechanical load into the equivalent thermal load and vice versa, of mechanical load to the equivalent thermal load. The first term in Eq. (1) represents the displacement induced by the mechanical load (F) while the second term represents the displacement due to the thermal load (ΔT). It can be seen from Eq. (1) that displacements, and thus the strains, induced by the mechanical load (F) and equivalent thermal load (ΔT_{eq}) given by Eq. (7) produce equal displacements and strains throughout the entire length of the end bearing pile. The actual thermal load (ΔT) can be expressed as

$$\Delta T = \eta\Delta T_{eq} \tag{8}$$

Furthermore, Eq. (7) implies that

$$F = AE\alpha\Delta T_{eq} \tag{9}$$

This study addresses only a compressive (F<0) mechanical load, thus implying that

$$\eta \begin{cases} > 0 \ cooling \\ = 0 mechnical\ load\ only \\ < 0 heating \end{cases} \tag{10}$$

The shaft friction force (Q_s) is obtained by integration of the shear stress along the soil pile interface that is expressed as

$$Q_s = -pk_s \int_0^L u(x)\,dx \tag{11}$$

The force at the pile tip is obtained by simply multiplying the axial stress developed at the pile tip with the cross-section area of the pile (A), thus resulting in

$$N_b = \sigma(0)A \tag{12}$$

By combining Eqs. (8), (9), (11) the thermo-mechanical shaft friction force for an end bearing energy pile is obtained as

$$Q_s = AE\alpha\Delta T_{eq}\left[(1+\eta)\left(\frac{1}{\cosh\psi L}-1\right)\right] \tag{13}$$

and combining Eqs. (8), (9), (2) and (12) gives the thermo-mechanical normal force at the pile tip as

$$N_b = AE\alpha\Delta T_{eq}\left[\frac{\eta(1-\cosh\psi L)+1}{\cosh\psi L}\right] \tag{14}$$

It follows from Eqs. (13) and (14) that the ratio of tip resistance to shaft resistance in end bearing energy piles is given by

$$\frac{N_b}{Q_s} = \frac{\eta}{1+\eta} - \frac{1}{(1+\eta)(\cosh\psi L - 1)} \tag{15}$$

Ratios of tip to shaft resistance for an energy pile subjected to thermo-mechanical loads represented by different η values are shown in Figure 1. In these analyses, dimensions and properties of the pile correspond to those encountered in the single energy pile constructed at the Swiss Federal Institute of Technology at Lausanne (Laloui et al. 2006). Thus, the length and the diameter of the pile are equal to 26 m and 1 m, respectively, while its elastic modulus and coefficient of thermal expansion are equal to 29.2 GPa and 1 × 10−5/°C, respectively. It is noted that the actual soil profile at the Swiss Federal Institute of Technology consists of four different soil layers located above the bedrock that were referred to as soils A1, A2, B, and C by Laloui et al. (2006). Thus, the soil profile used herein is hypothetical in that only a single soil is located above the bedrock. All of the four layers at this site were classified as low plasticity clays by Perić et al. (2017). While most of figures herein were developed for soil A1, some figures also include soil C. Knellwolf et al. (2011) used a finite difference method to model the response of the energy pile located at the Swiss Federal Institute of Technology. They reported the values of elastic shear spring stiffness representing soils A1 and C, which were determined from full-scale field tests, to be equal to 16.7 and 121.4 MPa/m, respectively. Therefore, soil A1 represents a soft clay layer, while soil C represents a stiff clay layer surrounding the pile. Using Eq. (5) results in ψ values equal to 0.0478/m and 0.1289/m for soils A1 and C respectively.

As shown in Figure 1, the load is transferred to the soil predominantly at the pile tip during heating (η <0). Specifically, N_b/Q_s is greater than one for η < -1, and tends to infinity as η approaches -1. At this value of η, the magnitudes of thermal and mechanical loads are equivalent while their directions are opposite, thus effectively cancelling the load transfer along the shaft. This always occurs in end bearing piles as η approaches -1 regardless of the soil type or pile properties.

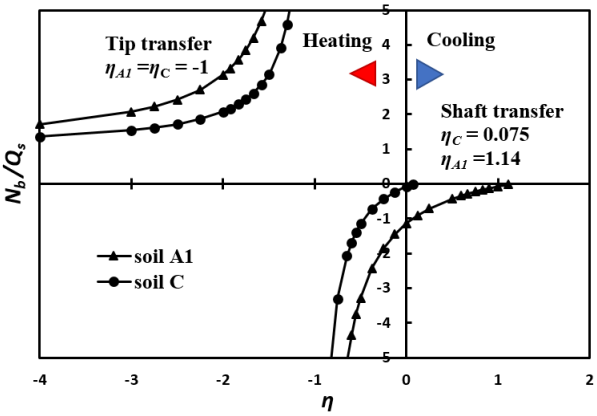

Figure1. Ratio of tip and shaft resistance for end bearing energy pile subjected to thermo-mechanical load versus η (soils A1 and C)

The corresponding shaft transfer mechanism is shown in Figure 2, where free body diagrams of an end bearing energy pile subjected to compressive mechanical load, and equivalent magnitude of heating (η = -1), as well as subjected to the combination of these two loads are shown.

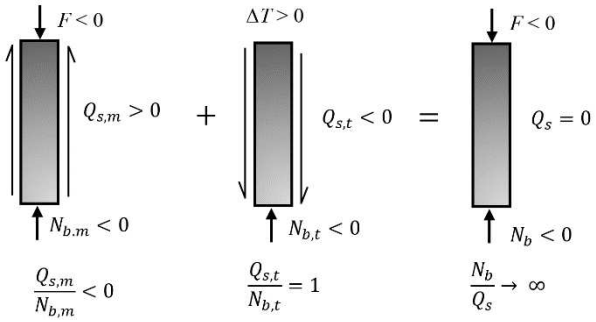

Figure 2. Free body diagrams of end bearing energy pile subjected to a) thermal, b) mechanical, and c) thermo-mechanical load (F< 0, tip transfer)

On the cooling side a certain combination of compressive mechanical load and amount of cooling will result in zero axial stress at the pile tip. This implies that the entire thermo-mechanical load is transferred along the pile shaft although the pile is an end bearing pile. The corresponding free body diagrams are depicted in Figure 3. This situation occurs at different load ratios (η) that depend on the soil type. In stiffer soil (C) this phenomenon occurs at a very low value of η (= 0.075) while soil A1 reaches the complete shaft transfer at much higher ratio of η (= 1.14).

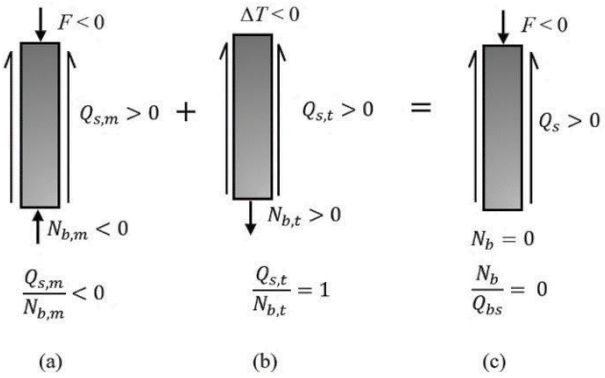

Figure 3. Free body diagrams of end bearing energy pile subjected to a) thermal, b) mechanical, and c) thermo-mechanical load (F < 0, shaft transfer)

Normalized shear stress and axial stress versus depth for different values of η are shown in Figures 4 and 5 that further illustrate the contribution of the pile tip and pile shaft resistance to load transfer mechanism.

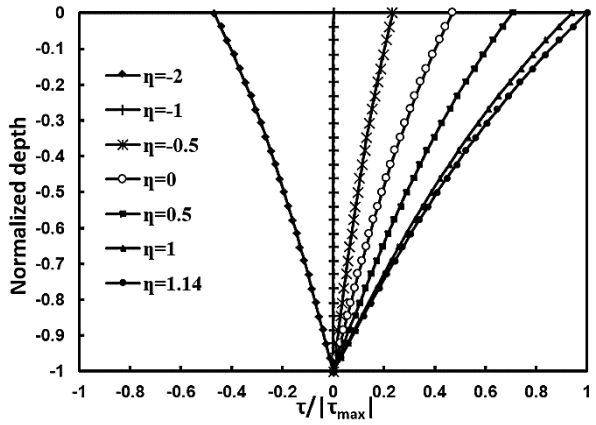

Figure 4. Normalized shear stress versus normalized depth for end bearing energy pile subjected to thermo-mechanical load for different values of η (soil A1)

As shown, in case that magnitudes of thermal and mechanical loads are equal (η = -1), there is absolutely no shear stress along the pile shaft and the load transfer occurs entirely through the pile tip while axial stress is constant throughout the depth. At η values greater than -1 the positive shear stress develops along the pile shaft, thus representing the upward acting shear stress along the pile shaft. Figure 5 shows that the axial stress at the pile head for all considered loading scenarios is constant. In case that η = -1 the axial stress at the pile head is equal to the axial stress at the pile tip and constant throughout the pile.

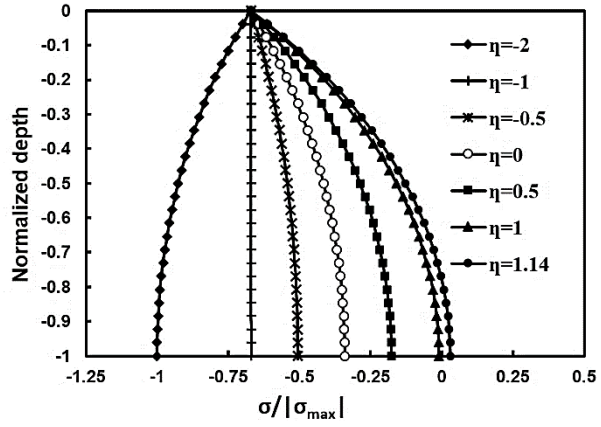

Figure 5. Normalized axial stress versus normalized depth for end bearing energy pile subjected to thermo-mechanical load for differen t values of η (soil A1)

3.2 *Load transfer mechanism in fully floating energy piles*

In fully floating piles there is no load transferred to the soil at the pile tip. Therefore, the tendency of the pile to expand or contract develops a zero-displacement point known as the null point. Saeidi Rashk Olia and Perić (2021a) and Saeidi Rashk Olia and Perić (2021c) developed the solutions for the locations of thermal and combined null points in semi floating and fully floating energy piles. In case of fully floating energy piles thermal null point is located at mid-length, thus resulting in the thermally induced shaft friction forces in the top and bottom half of the pile having equal magnitudes and opposite directions.

Similar to the end bearing pile the shaft friction force (Q_s) is obtained by integration of the shear stress along the soil pile interface. Thus, the top shaft friction force (Q_{ST}) and bottom shaft friction force (Q_{SB}) are obtained from

$$Q_{ST} = -pk_s \int_{\frac{L}{2}}^{L} u(x)\,dx \tag{16}$$

$$Q_{SB} = -pk_s \int_{0}^{\frac{L}{2}} u(x)\,dx \tag{17}$$

Combining g Eqs. (8), (9), (3), (16) and (17) the top and bottom shaft friction forces are obtained as

$$Q_{ST} = \frac{-AE\alpha\Delta T_{eq}}{\cosh(\frac{\psi L}{2})}\left[\eta\left(\cosh\left(\frac{\psi L}{2}\right)-1\right)-\frac{1}{2} + \cosh\left(\frac{\psi L}{2}\right)\right] \tag{18}$$

$$Q_{SB} = \frac{-AE\alpha\Delta T_{eq}}{\cosh(\frac{\psi L}{2})}\left[\eta\left(1-\cosh(\frac{\psi L}{2})\right)+\frac{1}{2}\right] \tag{19}$$

Based on Eqs. (18) and (19), the ratio of bottom to top shaft friction forces in the fully floating energy pile is given by

$$\frac{Q_{SB}}{Q_{ST}} = \frac{\eta\left(1-\cosh(\frac{\psi L}{2})\right)+\frac{1}{2}}{-\frac{1}{2}+\cosh\left(\frac{\psi L}{2}\right)+\eta\left(\cosh(\frac{\psi L}{2})-1\right)} \tag{20}$$

Figure 6 depicts Eq. (20) for different values of η. As shown, in a fully floating pile bottom shaft transfer occurs in compression and heating, whereby no shaft friction remains along the top half of the pile.

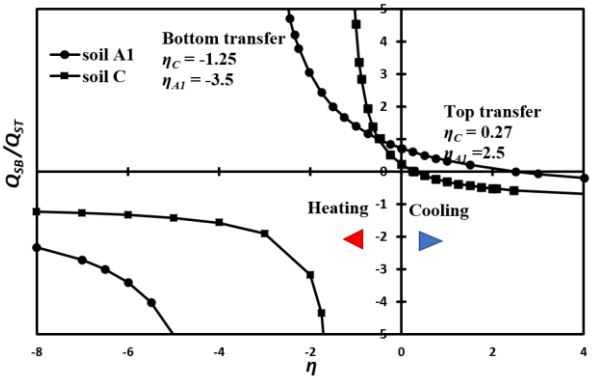

Figure 6. Ratio of bottom to top shaft resistance for a fully floating energy pile subjected to thermo-mechanical load versus η (soils A1 and C)

This is where the mechanically induced upward directed shaft friction on the top half of the pile (Figure 7a) is balanced with the downward directed thermally-induced shaft friction (Figure 7b) resulting from heating. Thus, the entire thermo-mechanical load in this case is transferred to the soil through the bottom half of the shaft. The emergence of this state is reliant on the soil type as demonstrated in Figure 6. Soil C develops a stiffer soil pile interface and reaches this stage at a lower amount of heating (η =-1.25). Soil A1 develops a softer soil pile interface and reaches this state at a higher amount of heating corresponding to η =-3.5.

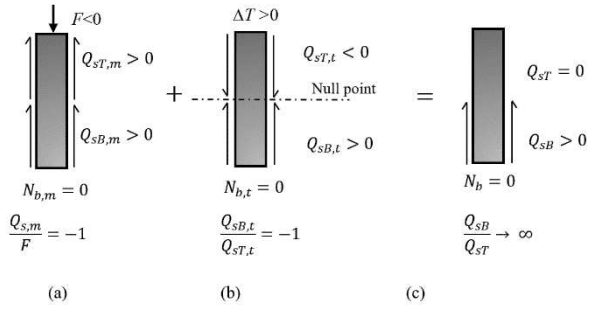

Figure 7. Free body diagrams fully floating energy pile subjected to a) thermal, b) mechanical, and c) thermo-mechanical load (F < 0, bottom transfer)

Once a fully floating pile is subjected to compression and cooling at some stage of thermal load, the upward directed mechanically-induced shaft friction (Figure 8a) is balanced with thermally induced downward directed friction (Figure 8b), thus resulting in the load being transferred to soil only along the top half of the pile shaft (Figure 8c). Similarly to the bottom shaft transfer, energy pile embedded in soil C reaches the top transfer stage at the lower amount of cooling (η = 0.27), while the pile embedded in soil A1 requires a larger amount of cooling (η = 2.5).

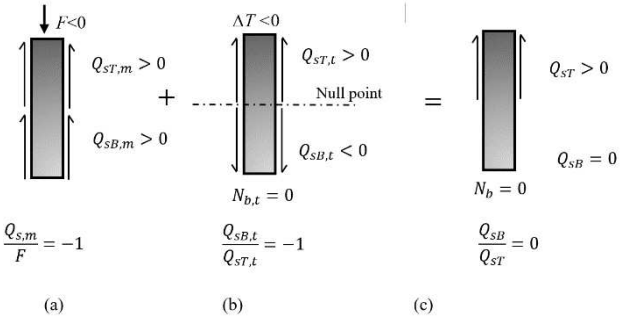

Figure 8. Free body diagrams fully floating energy pile subjected to a) thermal, b) mechanical, and c) thermo-mechanical load (F < 0, top transfer)

Normalized shear stress and axial stress along the pile shaft for a fully floating energy pile and different combinations of thermal and mechanical loads are shown in Figures 9 and 10, thus further illustrating the contribution of the pile shaft resistance to the load transfer mechanism.

Figure 10 highlights the absence of any resistance at the pile tip by demonstrating zero axial stress at the pile tip for all load combinations. The maximum compressive axial stress develops during heating (η =-3.5), which corresponds to bottom transfer case based on Figure 6. In case of top transfer (η =2.5) tensile axial stress develops approximately in the bottom half of the pile.

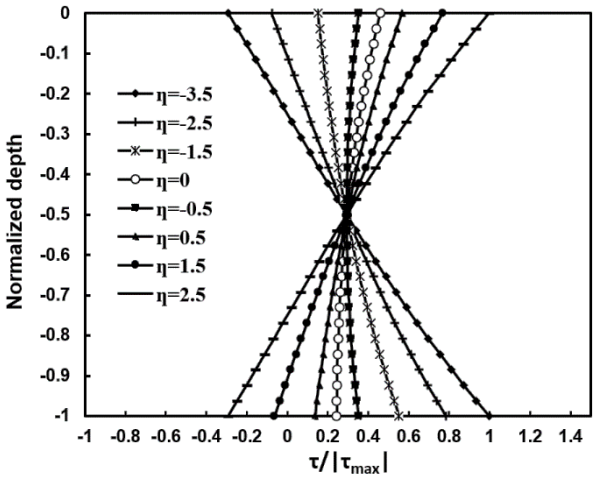

Figure 9. Normalized shear stress versus normalized depth for fully floating energy pile subjected to thermo-mechanical load for different values of η (soil A1)

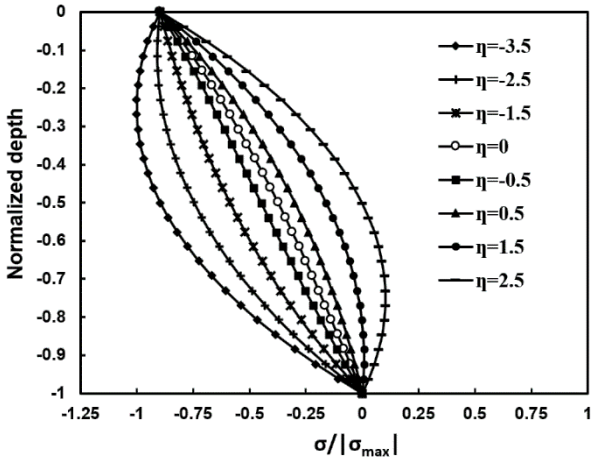

Figure 10. Normalized axial stress versus normalized depth for fully floating energy pile subjected to thermo-mechanical load for different values of η (soil A1)

4 CONCLUSIONS

This study investigated theevolution of a thermo-mechanical load transfer mechanism in single energy piles throughout a full heating-cooling cycle by implementing recently derived analytical solutions. The load transfer behaviors of end bearing and fully floating energy piles were studied, thus including the effects of end restraints on the response as well.

While the pile tip plays an important role in load transfer in end bearing piles it was shown that at some stage of cooling the load transfer at the tip can be fully eliminated, thus temporarily transforming an end bearing pile into a pile that transfers the entire thermo-mechanical load to the soil along its shaft. The amount of cooling required for this scenario to emerge depends on the soil type, the stiffer the soil the smaller the amount of cooling is required. Furthermore, in case that magnitude of heating is equivalent to the compressive mechanical load, the end bearing pile transfers the entire thermo-mechanical load to the soil or rock at its tip. At this state a constant thermo-mechanical axial stress develops in the pile.

Due to the absence of any tip resistance in fully floating energy piles top and bottom halves of the pile shaft play opposing

roles in transferring thermal load. Consequently, under a combined thermo-mechanical load the fully floating pile can reach the state whereby the net shaft transfer of load to the soil along its top half is eliminated. This can happen during heating. On the contrary with a proper amount of cooling the net shaft transfer along the bottom half of the pile can also be eliminated. During this state tensile stress can develop in the bottom half of the pile. Emergence of both of these states depends on the soil type, the stiffer the soil the smaller amount of heating or cooling is required to reach these states.

5 REFERENCES

Amatya, B. L., Soga, K., Bourne-Webb, P. J., Amis, T., and Laloui, L. 2012. Thermo-mechanical behaviour of energy piles. *Géotechnique*, 62(6), 503-519. doi.org/10.1680/geot.10.P.116

Bourne-Webb, P. J., Amatya, B., Soga, K., Amis, T., Davidson, C., and Payne, P. 2009. Energy pile test at Lambeth College, London: geotechnical and thermodynamic aspects of pile response to heat cycles. *Géotechnique*, 59(3), 237-248. doi.org/10.1680/geot.2009.59.3.237

Bourne-Webb, P. J., Amatya, B., and Soga, K. 2013. A framework for understanding energy pile behaviour. *Proceedings of the Institution of Civil Engineers-Geotechnical Engineering*, 166(2), 170-177. doi.org/10.1680/geng.10.00098

Cossel A. 2019. *Analytical solutionsf for thermo-mechanical soil structure interaction in energy piles*. Thesis submitted in partial fullfillment of the M.S. degree requirements, Kansas State University.

Goode, J. C., and McCartney J. S.. 2015. Centrifuge modeling of end-restraint effects in energy foundations.. *J. Geotech. Geoenviron. Eng*. 141 (8): 04015034. https://doi.org/10.1061/(ASCE)GT.1943-5606.0001333.

Iodice C., Di Laora R., and Madolini, A. 2020. Analytical Solutions for Ultimate Limit State Design of Thermal Piles. *Journal of Geotechnical and Geoenvironmental Engineering*, 146(5), 04020016, doi.org/10.1061/(ASCE)GT.1943-5606.0002204.

Knellwolf, C., Peron, H., and Laloui, L. 2011. Geotechnical analysis of heat exchanger piles. *Journal of Geotechnical and Geoenvironmental Engineering*, 137(10), 890-902. doi.org/10.1061/(ASCE)GT.1943-5606.0000513

Laloui, L., Nuth, M., and Vulliet, L. 2006. Experimental and numerical investigations of the behaviour of a heat exchanger pile. *International journal for numerical and analytical methods in geomechanics*, 30(8), 763-781. doi.org/10.1002/nag.499

Perić, D., Tran, T. V., and Miletić, M. 2017. Effects of soil anisotropy on a soil structure interaction in a heat exchanger pile. *Computers and Geotechnics*, 86, 193-202. doi.org/10.1016/j.compgeo.2017.01.005

Perić, D., Cossel, A. E., and Sarna, S. A. 2020. Analytical Solutions for Thermomechanical Soil Structure Interaction in End-Bearing Energy Piles. *Journal of Geotechnical and Geoenvironmental Engineering*, 146(7), 04020047. doi.org/10.1061/(ASCE)GT.1943-5606.0002269

Rotta Loria, A.F., and Laloui, L. 2018. Thermo-mechanical schemes for energy piles. *In International Symposium on Energy Geotechnics (pp. 218-225)*. Springer, Cham.

Saeidi Rashk Olia, A, and Perić, D. 2021a .Thermomechanical soil–structure interaction in single energy piles exhibiting reversible interface behavior. *International Journal of Geomechanics*, 21(5), 04021065. doi.org/10.1061/(ASCE)GM.1943-5622.0002014

Saeidi Rashk Olia, A, and Perić, D. 2021b. Effects of End Restraints on Thermo-Mechanical Response of Energy Piles. In *IFCEE 2021* (pp. 585-594). doi.org/10.1061/9780784483404.054

Saeidi Rashk Olia, A, and Perić, D. 2021c. Effects of Axial Load on the Location of a Combined Null Point in Energy Piles. In *IFCEE 2021 (pp. 595-604)*. doi.org/10.1061/9780784483404.055

Stewart, M. A., and McCartney, J. S.. 2014. Centrifuge modeling of soilstructure interaction in energy foundations. *J. Geotech. Geoenviron. Eng.* 140 (4): 04013044. doi.org/10.1061/(ASCE)GT.1943-5606.0001061